

Chapter 7

Summary and Future Scope

In this chapter, the overall summary of the work done and its outcome is presented. Also at the end, the future scope of the present work is discussed.

7.1 Summary of the present work

The samples of delafossite type oxides comprising of two series CuFeO_2 and CuCrO_2 have been successfully synthesized by using the conventional solid-state reaction. The CuFeO_2 series is prepared by doping Ti, Mn, Ga and V at the Fe site was prepared with the help of a cost-effective solid-state technique under a high vacuum. CuCrO_2 series doped with Mg, Ti, Mn, Ni, Ga, Nb and V at Cr sites were also prepared. The in-depth XRD analysis confirmed the good quality of the samples without any impurity phases with the rhombohedral structure having space group R-3m. For the pure and doped CuCrO_2 samples the structural parameters correlate more with the expected valance state-based hole or electron doping induced changes in the local electronic structure rather than ionic sizes. Crystallite size along with induced lattice strain was also determined from XRD patterns for both series. SEM micrographs confirm the good crystallinity along with well-defined grain boundaries for both the CuFeO_2 and CuCrO_2 series samples.

Minor shifts in the E_g and A_{1g} modes in Raman of CuFeO_2 samples were observed due to Ti and Mn doping. A Jahn-Teller distortion-related extra peak was observed around 500 cm^{-1} but with variable strength. Mössbauer's measurement at room temperature confirmed the presence of octahedron distortion and suggested the absence of Fe^{2+} or mixed valence. The optical band gap had no significant changes in these samples. The phase purity of these samples prepared through the cost-effective solid-state reaction under high vacuum was further confirmed by the FTIR, Raman, and Mössbauer studies. Raman studies showed strong local distortions in Mn, Ti and Fe doped CuCrO_2 samples which had not been reported earlier. In both E_u and A_{2u} IR, active modes removal of degeneracy is observed, related to T_o and L_o optical modes of vibrations in Mn, Ti, Nb, Ga and V doped CuCrO_2 samples. The doping of mixed/or di- or tetra-valent ions reduced the bandgap of CuCrO_2 samples. These observed reductions in the band gap are related to changes in p-d hybridizations coupled with Jahn-Teller distortions rather than changes in bond distances, crystallite size, or unit cell volumes.

The dc conductivity studies of the CuFeO_2 samples showed a decrease in resistivity with the partial doping of the Fe site which can be correlated to the changes in carrier concentration as well as mobility due to induced charges and MO_6 based distortions. Small-polaron-based conduction was exhibited by the pure and Ti-doped CuFeO_2 samples. Moreover, Jonscher's law-based calculations through the exponent 'n' values showed an increasing trend for both the samples confirming non-overlapping small polaron tunneling (NSPT) model-based behavior for conduction. The low-temperature electrical conduction behavior of CuCrO_2

samples is significantly altered with the electron or hole doping in these predominantly phonon-driven semiconducting systems. Here also a predominantly small polaron hopping process is established through ac conductivity studies. Jonscher's power law analysis here instead showed that for Ti and Mn-doped samples, the conductivity is attributed to the correlated barrier hopping model, while for samples with other substitutions it is related to the NSPT model.

The magnetic and dielectric studies for pure and Ti-doped CuFeO_2 samples demonstrate a significant role of Jahn–Teller effect-based local defects, particularly at low temperatures. The magnetization and dielectric permittivity measurements of the studied pure and doped CuCrO_2 samples showed clear evidence of magneto-dielectric coupling. Moreover, the optimization of the phonon-induced localized carrier hole density along with the reduction in helical disorder around MO_6 octahedra through suitable electron/hole doping is an effective way to enhance the double exchange along with the Cr-O-M-O linkages or superexchange between $\text{M}^{3+/4+}$ - Cr^{3+} mediated by oxygen at low temperatures. The present correlated study clearly highlights the role of doping level and local distortions in deciding the magnetic and multiferroic nature of this system providing an effective tool to tune its physical and chemical behavior.

7.2 Scope of the future works

Technological advances in the fields of optoelectronics, photonic and magnetic devices are incomplete without thin-film materials. In the form of thin films, the materials can be easily integrated into devices. The thermal stability and reasonably hard nature of thin films add to their usefulness. Semiconductors in the form of thin films are easy to study in terms of optical studies and charge concentration studies.

In the present samples due to large resistivity and inbuilt inhomogeneity when taken as pellets inconsistent results of Hall measurements were obtained. Such a problem can be solved with a well-characterized thin film. Also, X-ray absorption spectroscopy measurements can be performed for studying the fraction of transition metal cations in different spatial locations, their oxidation states, structural disorder, etc. Therefore, in order to obtain a better understanding of the present samples, some of the thin films have already been prepared using the pulsed laser deposition technique. The target for pulsed laser deposition was prepared in the form of a circular pallet of 10 mm. The XRD of one of the representative $\text{CuCr}_{0.96}\text{Mn}_{0.03}\text{V}_{0.01}\text{O}_2$ thin films is given in figure 7.1 below along with its Rietveld

refinement. The film was deposited on Si (100) substrate with a substrate temperature of 750 °C. The target to substrate distance was kept at 4.5 cm, laser energy and repetition rate were kept at 240 mJ/cm² and 10 Hz respectively. The base pressure of the deposition chamber was 5×10^{-5} mTorr. The oxygen partial pressure was maintained at 100 mTorr and deposition time was 30 min. The reliability factors, lattice constants and other relevant crystallographic data are given in table 7.1.

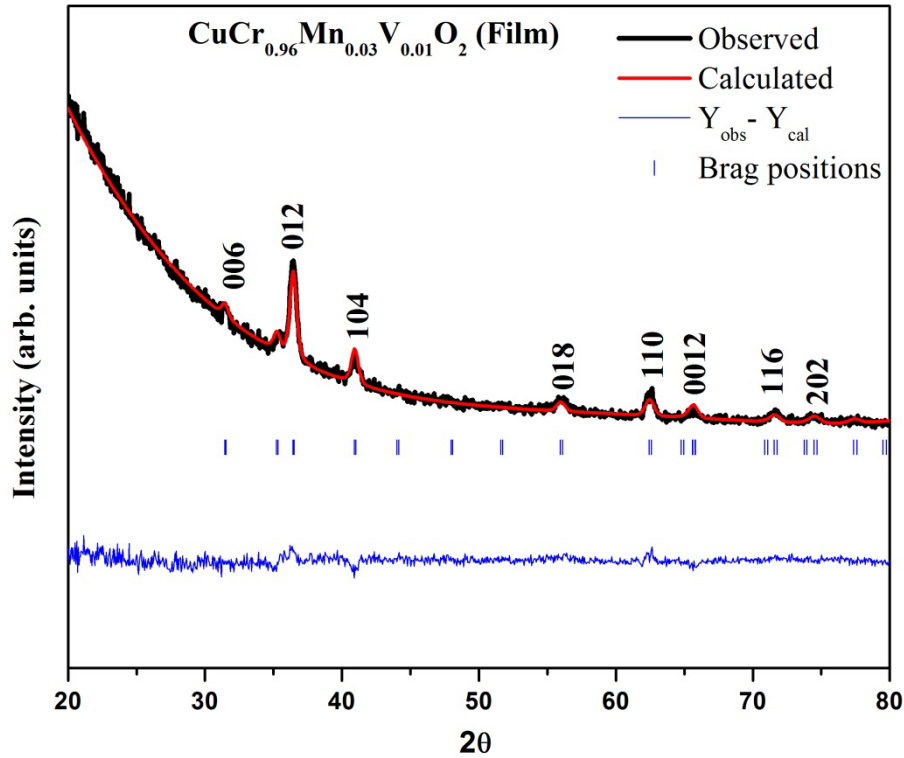


Figure 7.1: Experimental X-ray powder diffraction pattern (black line) and calculated pattern (red line) for $\text{CuCr}_{0.96}\text{Mn}_{0.03}\text{V}_{0.01}\text{O}_2$ thin film. The difference is given as a bottom line. The set of Bragg ticks (blue) corresponds to the $R\bar{3}m$ space group of delafossite.

Table 7.1: Crystallographic data for $\text{CuCr}_{0.96}\text{Mn}_{0.03}\text{V}_{0.01}\text{O}_2$ thin film

Space group	$R\bar{3}m$
$a = b$ (Å)	2.973(16)
c (Å)	17.060(9)
Volume (Å ³)	130.605
O (z)	0.07561
χ^2	1.52
S	1.23